Shifts in Ballistocardiography Fiducials Reflect Increases in Pulse Wave Velocity Measured by 4D-Flow MRI

Amin Hossein[1,2], Jérémy Rabineau[1,2] , Vitalie Faoro[1,2], Philippe van de Borne[1]

[1]Laboratory of Physics and Physiology, Department of Cardiology, Hôpital Erasme, Hôpital Universitaire de Bruxelles, Belgium
[2]Research Unit in Cardio-Respiratory Physiology, Exercise & Nutrition, Faculty of Human Movement Sciences, Université libre de Bruxelles, Belgium

Abstract

Arterial stiffness is a marker of vascular aging and an independent predictor of cardiovascular risk. Aortic pulse wave velocity (PWV), a proxy for arterial stiffness, increases during prolonged exposure to simulated microgravity such as head-down tilt (HDT) bed rest. We investigated whether these PWV changes are reflected in the timing of fiducial points in the ballistocardiogram (BCG), namely the I, J, and K waves. Data came from the AGBRESA study, where 24 healthy subjects underwent 60 days of strict -6° HDT. Prior 4D-flow MRI analyses showed a significant increase in aortic PWV from day 5 (HDT5) to day 56 (HDT56) (+16%, $p<0.001$). At all timepoints, wearable sensors recorded ECG, sternum seismocardiography (SCG), and lumbar BCG. Fiducial points corresponding to the aortic valve opening (AO) in SCG and I, J, and K waves in BCG were annotated relative to the ECG R peak. Comparison between HDT5 and HDT56 showed stable AO and I timings, while J and K waves occurred earlier. A linear mixed-effects model with random subject intercepts confirmed a significant association between 1/PWV and the I–K interval in BCG ($p<0.01$), independent of height or heart rate. These findings indicate that increased PWV is reflected in BCG temporal shifts.

1. Introduction

Arterial stiffness is a marker of vascular aging and an independent predictor of cardiovascular risk. It is associated with hypertension, coronary artery disease, atrial fibrillation, stroke, and heart failure [1][2]. Structural changes such as elastin degradation, collagen deposition, and calcification evolve silently over decades, often remaining undetected until irreversible cardiovascular damage occurs [3]. Early detection is therefore critical.

Pulse wave velocity (PWV), defined as the distance traveled by the arterial pressure wave divided by pulse transit time (PTT), is the gold-standard marker of arterial stiffness [4]. It directly reflects aortic compliance, making it more specific than classical risk factors. In particular, aortic PWV (Ao-PWV) captures the mechanical state of central arteries, which are most affected by age-related structural changes and wave reflections [5]. Ao-PWV has strong prognostic value and is recommended in risk assessment guidelines [5]. However, despite this relevance, routine PWV measurement remains uncommon. Invasive approaches are impractical, while non-invasive gold standards such as carotid–femoral tonometry, Doppler ultrasound, or cardiac MRI are expensive, complex, and limited to specialized centers. More accessible cuff-based devices exist but rely heavily on model-based estimations with limited physiological specificity. As a result, PWV is rarely measured longitudinally in general practice, precisely when early stiffening begins [6].

Ballistocardiography (BCG) and seismocardiography (SCG) offer a potential solution. These non-invasive, low-cost techniques capture mechanical vibrations of the cardiovascular system: BCG reflects the body's recoil to blood ejection, while SCG records chest wall vibrations linked to valve and myocardial events [7,8]. Specific fiducial points, such as aortic valve opening (AO) in SCG and the I, J, K waves in BCG, have been linked to central hemodynamic events [9]. The downward I wave is primarily generated by the acceleration of blood from the left ventricle into the ascending aorta [9]. This is followed by the upward J wave, which is associated with the changing direction of the pulse wave as it travels from the ascending aorta to the descending aorta [9]. Finally, the downward K wave was hypothesised to mainly correspond to the reflection of the pulse wave [9]. Unlike photoplethysmography (PPG)-based methods, which emphasize peripheral arteries, the SCG–BCG combination targets central mechanical events, potentially providing a stiffness index more directly influenced by aortic compliance.

Nevertheless, BCG and SCG remain underused due to motion artifacts and an incomplete understanding of signal

genesis. In controlled conditions such as bed rest, motion artifacts are minimal, offering an opportunity to isolate and validate physiologically meaningful fiducials. Importantly, no study has yet combined SCG and BCG to compare PWV estimates with 4D-flow MRI, a robust imaging modality that provides physiologically meaningful PWV estimates [10].

In this study, we investigated whether PWV changes observed during long-term -6° head-down tilt (HDT) bed rest, a model of cardiovascular deconditioning and simulated microgravity, are reflected in the timing of BCG fiducial points. We hypothesized that increased PWV would lead to earlier occurrences of the J and K waves relative to the BCG I wave, ECG R peak, and SCG AO. By linking SCG–BCG intervals with PWV quantified by 4D-flow MRI, we aimed to provide mechanistic validation of wearable-derived stiffness markers. Such an approach could enable beat-to-beat PWV monitoring in spaceflight and clinical prevention contexts, where routine assessment remains inaccessible.

2. Methods

2.1. Study Design and Population

The present analysis used data from the AGBRESA head-down bed rest study, jointly organized by NASA, ESA, and DLR, at the :envihab facility (DLR, Cologne, Germany) in 2019. A total of 24 healthy volunteers (8 women, median age 29 [26–38] years, body mass 74 [70–80] kg, body height 176 [167–182] cm) underwent 60 days of strict -6° HDT bed rest to simulate microgravity-induced cardiovascular deconditioning. The study aimed at comparing three groups with different regimes during the HDT period: daily 30-minute continuous or intermittent artificial gravity, or control. Individuals were randomized among the three groups; however, as no group effect was reported on cardiovascular parameters, data were pooled across all participants [11].

As described in our previous publication, aortic stiffness was assessed using 4D-flow cardiac MRI, which provides volumetric, time-resolved velocity fields in the thoracic aorta. Scans were acquired in horizontal position at 5 different time-points; at baseline 9 days before bed-rest (BDC-9), at 5, 21, and 56 days during HDT (HDT5, HDT21, HDT56, respectively), and 4 days after the beginning of recovery (R+4) on a 3T Biograph mMR scanner (Siemens, Erlangen, Germany). The sequence included free-breathing 4D flow with ECG and navigator gating, voxel size 2.4 × 2.4 × 2.0 mm^3, 20 cardiac phases per cycle, and velocity encoding of 150 cm/s. The thoracic aorta was semi-automatically segmented and centerlines extracted (CAAS MR Solutions 5.2.1, Maastricht, The Netherlands). A series of ~35 planes were reconstructed orthogonal to the centerline, from the sinotubular junction to the descending thoracic aorta, 12 cm distal to the bifurcation between the aorta and the left subclavian artery. PTT was estimated in the frequency domain between sequential planes, and Ao-PWV was obtained as the inverse slope of distance vs. PTT. A significant +16% increase in Ao-PWV was observed from HDT5 to HDT56 ($p < 0.001$) [11].

2.2. Recordings and Signal Processing

In the two hours preceding MRI, simultaneous ECG, SCG, and BCG were recorded in the supine position. Triaxial accelerometers and gyroscopes were attached at the sternum (SCG) and the lower back (BCG). Data were collected during resting, 6-second controlled breathing, and motionless conditions to minimize artifacts. Measurements were taken in a horizontal position at BDC-9 and R+4, and in the HDT position during the HDT period. The recording was 60 seconds long.

ECG was sampled at 200 Hz, while SCG and BCG were sampled at 50 Hz. R peaks were automatically detected on the ECG and subsequently verified visually. Ensemble averaging was performed for each signal, aligned to the R peak, as described in previous work [12]. For each subject and time point, fiducial points were annotated on the ensemble-averaged waveforms: AO and aortic valve closure (AC) in the dorso-ventral axis of SCG, and the I, J, and K waves in the caudo-cranial axis of BCG (Figure 1). All timings were expressed relative to the preceding ECG R peak. Intervals of interest included the time betwen AO and the reflected wave as measured by BCG (K); the time between I and J which represent the time for the blood wave to go from the ascending aorta to the descending aorta; the time between I and K which represent the time between the blood wave going from the ascending aorta and the reflected wave.

2.3. Statistical Analysis

Population means at HDT5 and HDT56 were compared to evaluate temporal shifts using a paired test. Associations between BCG-derived intervals and PWV were assessed using linear mixed-effects models with random subject intercepts to account for repeated measures. Inverse PWV was modeled as a function of BCG intervals. Height was included as a covariate, and additional models were tested to evaluate the contributions of BCG J timing, AO, and heart rhythm (HR). Model comparisons were performed using likelihood ratio tests and AIC/BIC criteria. Then, the repeated measures correlation coefficient (rrm) was used to determine the overall within-individual relationship. Results are reported as fixed-effect coefficients. Statistical significance was set at $p < 0.05$.

3. Results

A total of 119 recordings were available across all sessions, and all were analysable. Wearable lower-back BCG signals were of sufficient quality to consistently identify the I, J, and K waves in every subject. Figure 1 shows the ensemble-averaged median waveform at day 5 (HDT5, blue) and day 56 (HDT56, red) of -6° HDT bed rest, with fiducial points annotated.

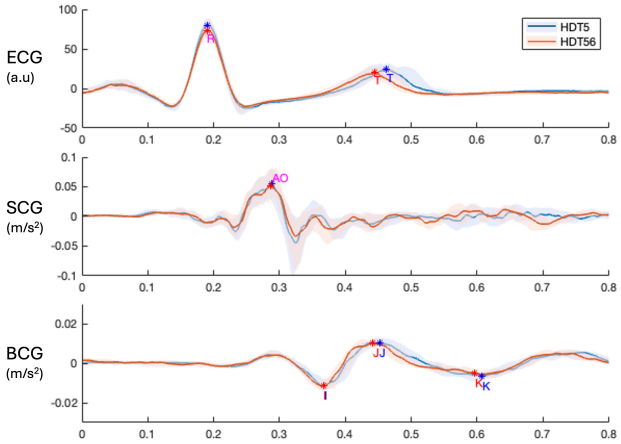

Figure 1. ECG, dorso-ventral SCG, and caudo-cranial BCG signals are shown for the median subject waveform at day 5 (HDT5, blue) and day 56 (HDT56, red) of -6° head-down tilt bed rest. The first quartile and third quartile of the waveforms are displayed with shadows around the median. Fiducial points are annotated: the aortic valve opening (AO) on SCG, and the I, J, and K waves on BCG.

Table 1 summarizes the group-level results. From HDT5 to HDT56, I–K interval decreased (232 [218–240] ms to 228 [217–245] ms, $p<0.05$), while HR increased markedly (58.8 [52.5–63.3] bpm to 74.8 [65.7–82.5] bpm, $p<0.01$). In contrast, Ao–K and I–J intervals did not show significant changes.

Table 1. PWV and time-interval metrics at successive timepoints. Medians and interquartile ranges.

Metric	BDC-9	HDT-5	HDT-56	R+4
PWV (m/s)	5.4 [4.7;6.0]	5.9 [5.3;6.9]	6.1 [5.6;6.9]	5.1 [4.4;6.0]
HR (bpm)	66.5 [60.2;75.3]	58.8 [52.5;63.3]	74.8 [65.7;82.5]	72.3 [63.6;81.4]
I-K (ms)	231 [218;254]	232 [218;240]	228 [217;245]	244 [222;259]
Ao-K (ms)	330 [310;359]	326 [308;349]	320 [302;340]	337 [309;358]
I-J (ms)	69.0 [64.0;77.5]	75.0 [69.5;80.5]	70.5 [64.0;77.0]	74.0 [65.0;80.8]

BCG I–K interval was positively associated with 1/PWV ($\beta = 0.00032$, $p = 0.015$), independent of height. Height showed a significant negative association with 1/PWV ($\beta = –0.189$, $p = 0.014$). In contrast, the RR interval was not a significant predictor ($p = 0.90$) and did not improve model fit. Subject-specific random effects were small but justified the inclusion of a random intercept. The addition of the AO as measured by SCG did not improve model fit either. Overall, the model confirmed that BCG I–K timing provides meaningful information about PWV beyond simple anthropometric variation.

Repeated-measures correlation analysis further supported this association: 1/PWV was significantly correlated with the I–K interval across all participants (rrm = 0.24 (0.20–0.29), $p < 0.01$; see Fig. 2). In addition, the I-J interval also correlated with 1/PWV (rrm = 0.22 (0.18–0.25), $p < 0.05$).

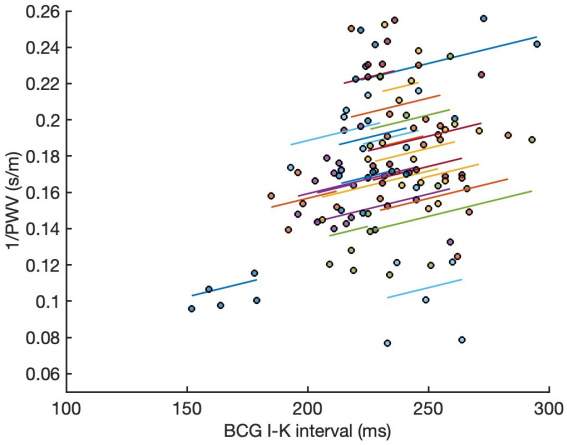

Figure 2. Relationship between ballistocardiography I–K interval and the inverse of pulse wave velocity (1/PWV). Each point represents an individual measurement, with regression lines fitted per subject (same color), indicating a positive association between I–K interval and 1/PWV.

4. Discussion

Our results demonstrate that a wearable accelerometer placed on the lower back provides high-quality BCG signals in all subjects, with clear and reproducible I–J–K waves. This is notable given the mixed evidence in prior work: while some studies reported difficulties obtaining consistent wearable BCG signals [9], others such as Etemadi et al. showed that wearable BCG waveforms can closely match those from standard force-plate systems [13]. In our analysis, higher aortic PWV assessed by MRI was associated with shorter I–K intervals on BCG. This relationship is physiologically consistent: the K wave has been hypothesized to correspond to the arrival of the reflected wave, which returns earlier when pulse wave velocity is higher due to stiffer arteries. Thus, the temporal shift of the K wave in the BCG provides a potential marker

of arterial stiffening. Importantly, this effect was observed using BCG alone, without the need for a distal sensor. in contrast to earlier approaches that combined BCG with PPG [14] or SCG with PPG [13] to derive pulse transit times.

Previous studies typically combined BCG with PPG [14] or SCG with PPG [13] to compute pulse transit times. For example, Yousefian et al. showed that wrist BCG combined with fingertip PPG correlates strongly with blood pressure [15], while Carek and Inan demonstrated that scale-mounted BCG can serve as the proximal anchor for carotid–femoral PTT [16]. SCG has also been explored for cuffless hemodynamics. For example, wearable patches ("SeismoWatch" devices) capture the aortic valve opening via SCG and use it as the proximal pulse timing reference [13]. Our approach is distinct in that it relies solely on wearable BCG fiducials, without requiring a peripheral PPG channel. Moreover, in our dataset, the addition of SCG intervals did not improve correlation with PWV, underscoring that the dominant stiffness information was already present in the BCG signal. A limitation of the study is that PWV and BCG measurements were not obtained simultaneously, although they were collected within less than two hours of each other. Moreover, PWV was assessed by MRI in the horizontal position, whereas BCG recordings during the bedrest period were performed in the -6° HDT position. This, together with the relatively small sample of young healthy adults, may have attenuated the strength of the observed associations. The BCG signal sampling frequency of 50 Hz is also a limitation, as a higher sampling frequency will probably lead to better precision of the fiducial points. Further studies in larger and more heterogeneous populations, ideally with simultaneous BCG and reference PWV acquisition, are warranted.

A natural extension of this work is the development of a physiologically grounded model for PWV estimation based on scaling laws. Such a framework could integrate BCG-derived fiducials with SCG-based cardiac timings (e.g., AO, LVET), heart rate, and anthropometric variables such as body surface area and height. This multimodal approach would not only improve the robustness of wearable stiffness monitoring but may also allow discrimination between central aortic PWV (e.g., I–J interval) and composite central–peripheral PWV (e.g., I–K interval).

Acknowledgments

We would like to thank the entire team at the DLR for managing the entire study, as well as Kerstin Kempter and Annette von Waechter for generating the cardiac MRI data.

References

1. Ben-Shlomo Y, Spears M, Boustred C, May M, Anderson SG, Benjamin EJ, et al. Aortic pulse wave velocity improves cardiovascular event prediction: an individual participant meta-analysis of prospective observational data from 17,635 subjects. J Am Coll Cardiol. 2014 Feb 25;63(7):636–46.
2. Vlachopoulos C, Aznaouridis K, Stefanadis C. Prediction of cardiovascular events and all-cause mortality with arterial stiffness: a systematic review and meta-analysis. J Am Coll Cardiol. 2010 Mar 30;55(13):1318–27.
3. Mitchell GF, Hwang SJ, Vasan RS, Larson MG, Pencina MJ, Hamburg NM, et al. Arterial stiffness and cardiovascular events: the Framingham Heart Study. Circulation. 2010 Feb 2;121(4):505–11.
4. Smulyan H, Mookherjee S, Safar ME. The two faces of hypertension: role of aortic stiffness. J Am Soc Hypertens. 2016 Feb;10(2):175–83.
5. Townsend RR, Wilkinson IB, Schiffrin EL, Avolio AP, Chirinos JA, Cockcroft JR, et al. Recommendations for improving and standardizing vascular research on arterial stiffness. Hypertension. 2015 Sept;66(3):698–722.
6. Vlachopoulos C, Aznaouridis K, Stefanadis C. Prediction of cardiovascular events and all-cause mortality with arterial stiffness: a systematic review and meta-analysis. J Am Coll Cardiol. 2010 Mar 30;55(13):1318–27.
7. Inan OT, Migeotte PF, Park KS, Etemadi M, Tavakolian K, Casanella R, et al. Ballistocardiography and seismocardiography: a review of recent advances. IEEE J Biomed Health Inform. 2015 July;19(4):1414–27.
8. Starr I. The relation of the ballistocardiogram to cardiac function. The American Journal of Cardiology. 1958 Dec 1;2(6):737–47.
9. Rabineau J, Nonclercq A, Leiner T, van de Borne P, Migeotte PF, Haut B. Closed-loop multiscale computational model of human blood circulation. applications to ballistocardiography. Front Physiol. 2021 Dec 9;12.
10. Markl M, Wallis W, Strecker C, Gladstone BP, Vach W, Harloff A. Analysis of pulse wave velocity in the thoracic aorta by flow-sensitive four-dimensional MRI: reproducibility and correlation with characteristics in patients with aortic atherosclerosis. J Magn Reson Imaging. 2012 May;35(5):1162–8.
11. Rabineau J, Issertine M, Hoffmann F, Gerlach D, Caiani EG, Haut B, et al. Cardiovascular deconditioning and impact of artificial gravity during 60-day head-down bed rest-Insights from 4D flow cardiac MRI. Front Physiol. 2022;13:944587.
12. Hossein A, Rabineau J, Gorlier D, Pinki F, van de Borne P, Nonclercq A, et al. Effects of acquisition device, sampling rate, and record length on kinocardiography during position-induced haemodynamic changes. BioMedical Engineering OnLine. 2021 Jan 6;20(1):3.
13. Etemadi M, Inan OT. Wearable ballistocardiogram and seismocardiogram systems for health and performance. J. Appl. Physiol. 2018 Feb 1;124(2):452–61.
14. Kříž J, Šeba P. Force plate monitoring of human hemodynamics. Nonlinear Biomed Phys. 2008 Feb 22;2:1.
15. Yousefian P, Shin S, Mousavi A, Kim CS, Mukkamala R, Jang DG, et al. The potential of wearable limb ballistocardiogram in blood pessure monitoring via pulse transit time. Sci Rep. 2019 July 23;9(1):10666.
16. Carek AM, Inan OT. Robust sensing of distal pulse waveforms on a modified weighing scale for ubiquitous pulse transit time measurement. IEEE Trans Biomed Circuits Syst. 2017 Aug;11(4):765–72.

Address for correspondence:
Amin Hossein
Route de Lennik 808, 1070
Andelecht, Belgium
Amin.hossein@ulb.be